

Determining isotopy classes of crossing arcs in alternating links

Anastasiia Tsvietkova

Abstract. Given a reduced alternating diagram for a link, we obtain conditions that guarantee that the link complement has a complete hyperbolic structure, and every crossing arc is isotopic to a simple geodesic. The latter was conjectured by Sakuma and Weeks in 1995, and was previously proved only for 2-bridge links. Our conditions also ensure that crossing arcs are the edges of an ideal geodesic triangulation. We provide infinite families of closed braids for which our conditions hold.

Key words and phrases: alternating link, link complement, hyperbolic structure, geodesic

MSC 2010: 57M25, 57M50

1. Overview

A link diagram provides a combinatorial description of a topological object, a link complement in S^3 . A natural question arising from this description is whether the complement can be endowed with a complete hyperbolic structure. This question is connected with the question of the existence of an ideal geodesic triangulation of the complement. While both of these questions can often be answered after tedious computations for a particular link, it is not *a priori* clear what would be a successful choice of edges for such a triangulation.

In this note, we show that under certain conditions (that can easily be checked) the crossing arcs of a reduced alternating diagram are the edges of an ideal geodesic triangulation. By a crossing arc we mean a cusp-to-cusp arc traveling from the underpass to the overpass of a crossing. The triangulation obtained induces the complete hyperbolic metric on the link complement (which implies, in particular, that the link is hyperbolic without a reference to Geometrization). It follows that, under these conditions, crossing arcs are isotopic to simple geodesics. We provide examples for which this holds, including an infinite family of links.

This question has a long history. W. Thurston noticed that if we choose a decomposition of a hyperbolic link complement into two polyhedra, where the edges are crossing arcs of a link diagram, then we often obtain an ideal geodesic triangulation from it by subdividing the polyhedra ([14]). The method was generalized by Menasco for alternating links ([10]), and by Petronio beyond alternating ([11]). While this suggests that the arcs are often isotopic to geodesics, the procedure fails to provide an ideal geodesic triangulation with positive-volume tetrahedra in general. On the other hand, Sakuma and Weeks conjectured that crossing arcs of a reduced alternating diagram are the arcs of the canonical cell decomposition of the link complement ([13]), which would imply they are isotopic to geodesics. Their conjecture was proved for hyperbolic 2-bridge links in [3] and independently in [7] (see also Appendix to [6]), but has not been established for any wider classes of links.

Beyond 2-bridge links, there are few additional results that identify cusp-to-cusp arcs in link complements with certain topological or combinatorial description as geodesics. These are the examples of canonical cell decompositions by Sakuma and Weeks that imply that crossing arcs of some families of symmetric alternating links are isotopic to geodesics (see Examples I.2.2-I.2.4 in

[13]), and work of Adams, Burton, Cooper, Futer, Purcell, and Reid that provides information about isotopy classes of certain tunnel arcs under additional restrictions ([1, 2, 4, 5]).

The sufficient conditions we obtain turn out to have a simple geometric interpretation. Let us return to the polyhedral decomposition suggested by Thurston and described by Menasco for alternating links. The term “polyhedron” is used only in topological sense here, since even for a hyperbolic link the faces might not be planar, *i.e.* might not lie in one hyperbolic plane. We will call such a polyhedron *cross-sectionally convex*, if at every ideal vertex all interior angles of a cross-section are in $(0, \pi)$. Note that this is not equivalent to the usual convexity: the faces might still be non-planar and, when subdivided, might yield a non-convex polyhedron.

Our conditions imply cross-sectional convexity of the two polyhedra suggested by Thurston. Then we show that every cross-sectionally convex polyhedral decomposition can be subdivided into an ideal geodesic *partially flat* triangulation (“partially flat” means that some, but not all tetrahedra have 0 volume, while the rest have positive volume). In particular, for links satisfying our conditions the purely combinatorial algorithm described by Thurston, Menasco and Petronio provides an ideal geodesic partially flat triangulation that induces the complete hyperbolic structure on the link complement. Such triangulations appear to be useful for various other purposes as well (see, for example, [9]).

The following is a short overview of our methods and techniques. In [15, 16], Morwen Thistlethwaite and the author introduced an alternative way of parameterizing hyperbolic structures of links. It uses complex labels assigned to a link diagram that describe horoball structures in \mathbb{H}^3 . We will refer to these labels as to *diagram labels*. The triangulation is not performed, and instead the method uses isometries of preimages of polygons bounded by the regions of the link diagram. This results in a set of relations, to which we will refer as to *hyperbolicity relations*.

In [15], we start with a hyperbolic link, and then describe the relations for the diagram labels merely as a convenient method for computing the (already existent) complete hyperbolic structure of the complement. In this paper instead we start with an arbitrary link diagram and the complex labels that satisfy the hyperbolicity relations for this diagram, and then establish additional conditions on the labels that guarantee the existence of the induced complete hyperbolic structure.

The paper is organized as follows. In Section 2, we describe the setting, developing a model that gives the complete hyperbolic structure based on the diagram labels rather than a triangulation process. In Section 3, we lay out and explain the conditions on diagram labels sufficient for our purposes, and prove that under these conditions, the Thurston-Menasco polyhedral decomposition is properly embedded in \mathbb{H}^3 . In Section 4, we show that, further, the decomposition yields an ideal partially flat geodesic triangulation, and use this to conclude that a link complement has a complete hyperbolic structure. In section 5, we prove that crossing arcs are isotopic to simple geodesics under our conditions. Section 6 gives examples for which this holds (including infinite families of links), demonstrating that one can check the conditions from a link diagram. The families of links are different from the links provided by Sakuma and Weeks in [13].

2. Diagram labels

Consider the complement of a link L in S^3 , and a diagram D of L . In what follows, we will describe the correspondence between the points on the peripheral boundary of $S^3 - L$ and the points in the boundary of \mathbb{H}^3 through a solution of the hyperbolicity equations, introduced in [15]. In further sections, we will investigate under which conditions on the labels this correspondence yields the complete hyperbolic structure and the developing map for the manifold $S^3 - L$.

Every region R of D that is incident to at least three crossings may be viewed as a disk bounded by the geodesic arcs traveling from the overpass to the underpass at every crossing of R , and by the arcs traveling on the boundary torus from one crossing of R to the next crossing of R (black and gray arcs on Fig.1, left, respectively, where a region incident to three crossings is depicted). Every arc can be assigned a complex number - a diagram label. When the complete hyperbolic structure exists on $S^3 - L$, the diagram labels are called crossing and edge labels respectively, and they parameterize the hyperbolic structure (see [15] for details and geometric definitions of the labels).

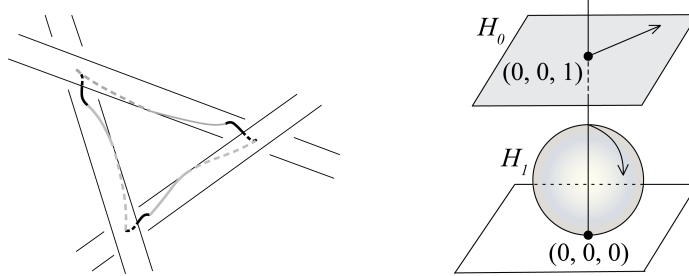


Fig.1

Hyperbolicity relations are two sets of polynomial relations in the diagram labels. The first set, called the region relations, guarantees that the composition of hyperbolic isometries rotating a preimage in \mathbb{H}^3 of the boundary of each disk, corresponding to a region of the diagram, must be the identity. If the region is 2-sided (*i.e.* it is a bigon), the two edge labels inside it are set to 0, and the two crossing labels are set equal, which corresponds to having no disk, but rather two homotopic geodesic arcs at crossings. The second set of relations (called the edge relations) for alternating links consists of relations of the form either $u = v \pm 1$ or $u = v$, where u, v are two edge labels assigned to two different sides of the same edge of D . By an edge of D we mean a segment from a crossing to the next crossing, and hence u and v lie in two different regions of D separated by this segment. The edge relations guarantee that whenever two arcs on the boundary torus form a simple closed curve going around a strand of L , the curve is homotopic to a meridian of length 1. We refer the reader to [15] for further details and examples.

Assume that there is a complex solution \bar{x} to the hyperbolicity relations for D (it is possible that all entries of \bar{x} have 0 imaginary part, and therefore are real). In particular, if there are n crossings in D , \bar{x} consists of n crossing labels w_1, w_2, \dots, w_n , and $2n$ edge labels u_1, u_2, \dots, u_{2n} .

Locally, every cusp (a neighborhood of a boundary torus for every link component) can be endowed with a Euclidean structure. At an overpass or an underpass of a crossing of D , choose a cusp cross-section with a unit meridian. We will now describe the correspondence between the link complement and a picture that, for a hyperbolic link complement, will later prove to be its preimage in \mathbb{H}^3 . Let the cusp cross-section correspond to an infinite union of Euclidean planes in this picture, and let the unit meridian correspond to the real number 1 on each of them. We will view each of these planes in the Euclidean three-dimensional space as a sphere minus the South pole, touching the plane $z = 0$ from above. We may consider these spheres as horospheres in \mathbb{H}^3 , using the upper half-space model of $\mathbb{H}^3 = \{(x, y, z) | z > 0\}$.

In what follows, we will connect the points where the horospheres are tangent to the plane $z = 0$ (we call such a point P_i the center of the corresponding horosphere H_i) by hyperbolic geodesics. We will situate and scale the horospheres so that the geometric definitions of the diagram labels are satisfied, even though the link L might not be hyperbolic. For this, we use a correspondence

between the points P_i on the boundary of \mathbb{H}^3 and the points \bar{P}_i on the boundary torus of $S^3 - L$. In particular, for each overpass or underpass of D we consider one point \bar{P}_i on the boundary torus, and a horosphere centered at a corresponding point P_i on the boundary of \mathbb{H}^3 .

To specify the size and the exact location of the horospheres, consider a region R_0 of D that has at least three crossings (and hence R_0 is not a bigon). Consider two consecutive crossings. The overstrand of the first crossing corresponds to a point P_0 on the boundary of \mathbb{H}^3 , and a horosphere H_0 centered at P_0 . A crossing arc runs to an understrand, corresponding to the point P_1 on the boundary of \mathbb{H}^3 , and horosphere H_1 . The overstrand of the next crossing corresponds to the same point P_1 on \mathbb{H}^3 , and the same horosphere. A crossing arc runs from there to an understrand corresponding to P_2 on the boundary of \mathbb{H}^3 , and horosphere H_2 . In \mathbb{H}^3 , connect points P_0 and P_1 , centers of H_0 and H_1 , by the hyperbolic geodesic γ_1 . Connect points P_1 and P_2 by a geodesic γ_2 . Denote the preimage of the meridian on the horosphere H_i by m_i throughout.

Let the crossing label that corresponds to the same crossing of D that γ_1 does, be w_1 of \bar{x} . If w_1 is 0, then the centers of the horospheres H_0, H_1 coincide, γ_1 is null-homotopic, and we can proceed to the next horosphere. So let us assume that this crossing label is not 0.

Place one of the horospheres, H_0 , as an “infinite” horosphere, the plane $z = k$. Introduce the coordinates for \mathbb{H}^3 (i.e. for the Euclidean 3-dimensional upper half-space $\{(x, y, z) \mid z > 0\}$) so that $k = 1$, and the preimage of m_0 is the unit vector going from $(0, 0, 1)$ to $(1, 0, 1)$. Place H_1 at the point $(0, 0, 0)$ (as on Fig.1, right, the horospheres are shaded). We may assume that P_0, P_1 are distinct, since otherwise $|w_1| = 0$ (which happens if and only if $w_1 = 0$). Scale H_1 in \mathbb{H}^3 so that $|w_1|$ is the Euclidean diameter of H_1 . Additionally, rotate H_1 so that the angle by rotation between m_0 and m_1 is $\arg w_1 - \pi$. The horospheres H_0, H_1 are now situated so that the geometric definition of the crossing label w_1 from [15] is satisfied.

The geodesic γ_2 is uniquely defined by one of its endpoints, P_1 , and the corresponding edge label u_2 which tells where γ_2 pierces H_1 . In particular, m_1 , which is the preimage of a meridian on H_1 , determines the unit distance and direction of the unit translation on H_1 . The complex number u_2 (possibly, with a negative sign, depending on whether the direction of our travel along the region of D corresponds to an orientation we choose for the link) is the translation on H_1 from the point where γ_1 pierces H_1 to the point (say, M_1) where γ_2 pierces H_1 . Hence we obtain the position of M_1 on H_1 . Two points, P_1 and M_1 , uniquely determine the geodesic γ_2 and therefore determine the position of the other endpoint P_2 of γ_2 .

The diameter of H_2 centered at P_2 and the direction of m_2 is determined by the next crossing label, w_2 . Proceeding similarly from a horosphere to horosphere, region by region, we obtain a uniquely defined and scaled collection of horoballs with geodesics connecting them, a coordinate system on \mathbb{H}^3 and Euclidean coordinates on each horosphere such that the preimage of every meridian corresponds to the real number 1.

Since the link L is not necessarily a hyperbolic link, the described process might lead to certain degeneracy. For example, the picture may consist of a single horosphere, if all the labels are 0. In the next sections we will prove that this set-up together with a few additional conditions on the labels induce a complete hyperbolic metric on $S^3 - L$.

3. Decomposition into two properly embedded polyhedra

In this section, we consider a decomposition of the alternating link complement $S^3 - L$ into two ideal polyhedra, $\bar{\Pi}_1, \bar{\Pi}_2$, one above the reduced alternating diagram D of L , and one below, as described by Menasco in [10]. Assume additionally that the diagram D is twist reduced in the

sense of [8]. Every alternating link admits such a diagram (see Section 3 in [8] for the definition and explanation).

The polyhedra are topological, and do not necessarily agree with the hyperbolic structure (which, possibly, does not even exist). However, the decomposition corresponds to the ideal polyhedra Π_1, Π_2 with straightened edges in \mathbb{H}^3 in the following way. In Section 2, we described the correspondence between points on the boundary of \mathbb{H}^3 and points on the boundary tori at overpasses/underpasses of L using the diagram labels. This gives the correspondence between the vertices of $\bar{\Pi}_i$ and the vertices of Π_i , $i = 1, 2$. By “straightened edges” we mean that every arc α of the decomposition of $S^3 - L$, that connects two points on the boundary torus of L (say, points \bar{P}_1 and \bar{P}_2), corresponds to the geodesic γ connecting the corresponding points P_1, P_2 in the boundary of \mathbb{H}^3 . Denote the set of such geodesic edges of Π_i by \mathcal{E}_i .

Remove the vertex of Π_i situated at infinity, and all edges of \mathcal{E}_i incident to it, and denote the remaining collection of vertices and edges by $\mathcal{E}_i - \{v\}$. In the upper half-space model of \mathbb{H}^3 , let f be the vertical projection of $\mathcal{E}_i - \{v\}$ onto the plane $z = 0$. A fragment of such a projection can be seen on Fig.4, right, with edges of the polyhedron in gray and their image in black.

Consider a collection of edges and vertices in \mathbb{H}^3 corresponding to a face \bar{F} of $\bar{\Pi}_1$. Denote this collection by \bar{F} and assume that \bar{F} does not contain a vertex at infinity. The ideal vertices of \bar{F} (denote all of them by v_1, v_2, \dots, v_j) do not necessarily lie in one hyperbolic plane. We may however introduce a “straightened” face F as follows.

By taking the projection $f(\bar{F})$, we obtain a polygon in the plane $z = 0$. It is not necessarily a simple polygon, *i.e.* its edges might intersect. There is however at least one simple polygon whose boundary includes at least one edge of $f(\bar{F})$. For every such simple polygon (say, $f(W'_i)$), there is an ideal polygon W'_i consisting of edges and ideal vertices of Π_i . Let the vertices of W'_i be v_1, \dots, v_b , and let the horospheres centered at them be H_1, \dots, H_b respectively. The size of the horospheres for a particular link is determined by the diagram labels, as described in the previous section. Now denote by W_i the truncated polygon bounded by two types of arcs. An arc of the first type is a segment of a hyperbolic geodesic arc between a point on a horosphere H_k (denote the point by M_k) to a point on a horosphere H_{k+1} (denote the point by N_{k+1}), $k = 1, 2, \dots, b - 1$. Every such hyperbolic geodesic arc coincides with an edge of the ideal polygon W'_i . The second type is an arc traveling on a horosphere H_k and connecting the points N_k, M_k , $k = 1, 2, \dots, b$. For every such truncated polygon W_i , fix a finite (*i.e.* non-ideal) triangulation t_i whose vertices are the points M_k, N_k on H_k , $k = 1, 2, \dots, b$. Let t_i be such that for every its edge e'_j not in \mathcal{E}_i ($i = 1, 2$), $f(e'_j)$ is entirely within one of the simple Euclidean polygons bounded by the images of edges of \bar{F} from \mathcal{E}_i under f . For every W_i , there is more than one such triangulation; we choose t_i so that the restriction of f to every triangle is bijective, if such a triangulation exists.

The vertices v_1, \dots, v_j of \bar{F} are centers of the horospheres H_1, \dots, H_j , whose sizes are defined by the corresponding diagram labels as explained in the previous section. For a vertex v_i of \bar{F} and two edges e_j, e_{j+1} of \bar{F} incident to v_i , let F coincide with the hyperbolic plane defined by e_j, e_{j+1} in the horoball neighborhood of v_i bounded by H_i . Consider a triangle T from one of triangulations t_i . If T is adjacent to a part of a face F that lies inside a horoball (as defined in the previous paragraph), let T be a part of F . If T is not adjacent to any such part of any face, let T be a part of any face to which it is adjacent along its other edges. This process defines F , which we call a “straightened face” of Π_1 .

Note that there is a hyperbolic isometry that moves v away from infinity, and places another vertex of Π_1 there. It can be used to choose the triangulation and therefore straightening of the remaining face of Π_1 . Face identifications of Π_1 and Π_2 together with the choice of straightening

of faces of Π_1 determine straightened faces of Π_2 . The collection of vertices, straightened edges and straightened faces of a polyhedron Π_i will be denoted by $\partial\Pi_i$, and, when we want to exclude the vertex at infinity and adjacent edges and faces, by $\partial\Pi_i - \{v\}$. Extend f to be the vertical projection of $\partial\Pi_i - \{v\}$ onto the plane $z = 0$. When we write Π_i , $i = 1, 2$, throughout, we mean either an ideal hyperbolic polyhedron bounded by $\partial\Pi_i$, or a corresponding truncated polyhedron with cross-sections lying on the horospheres centered at the ideal vertices. Since the meaning will be clear from the context, we will use the same notation in both cases.

Below we formulate the conditions on the diagram labels that guarantee that the cusped polyhedra are properly embedded in \mathbb{H}^3 . The conditions might seem unwieldy, but we will see that they have a simple geometric meaning. Here and further we assume that the diagram labels satisfy the hyperbolicity equations.

a) Consider labels on two sides of an overpass of a crossing. There are four such labels, $u, v, u+1, v+1$. Moving in the direction of the link orientation along the overpass, suppose the labels $u, u+1$ come last, as in Fig.2. Then $\text{Im } u > 0$ holds iff u is on the right with respect to our travel (Fig.2, left), and $\text{Im } u < 0$ holds iff it is on the left (Fig.2, right). This condition only needs to be checked for one arbitrarily chosen edge label of D that is not purely real (if there is such a label).

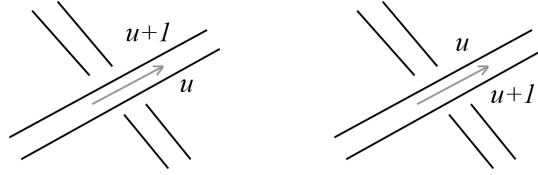


Fig.2

b) For every overpass/underpass that has two consecutive edge labels u, v (Fig.3, left), and is not incident to a bigon, either $\text{Im}(-(v+1)/u) > 0$ and $\text{Im}(-(u+1)/v) > 0$ hold if $\text{Im } u > 0$, or $\text{Im}(-v/(u+1)) > 0$ and $\text{Im}(-u/(v+1)) > 0$ hold if $\text{Im } u < 0$.

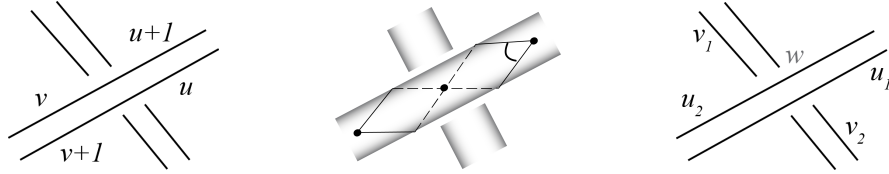


Fig.3

c) There exists a crossing of D for which the following holds. Suppose w is the crossing label assigned to the crossing, and $u_i, i = 1, 2$, are two edge labels on the adjacent overpass, and $v_j, j = 1, 2$ are two edge labels on the adjacent underpass (Fig. 4, right). Then at least one of the fractions $\frac{w}{u_i v_j}, \frac{w}{u_i(v_j+1)}, \frac{w}{v_j(u_i+1)}$ is not purely real for some i, j .

We will now explain the nature of these conditions.

Lemma 3.1. Conditions (a) and (b) imply the polyhedra Π_1 and Π_2 are cross-sectionally convex. Condition (c) guarantees that at least four horospheres are not all in the same plane, and not all crossing labels are 0.

Proof. In the polyhedron $\Pi_i, i = 1, 2$, there are at most four edges of \mathcal{E}_i incident to an ideal vertex. The cross-section determined by these edges is often a Euclidean quadrilateral. The

exception is a cross-section at an ideal vertex that has at least one incident polyhedral edge resulting from a bigon of D . Such a cross-section might be a triangle, or even a bigon that degenerates eventually into just one edge.

Consider a quadrilateral cross-section. One may see one such cross-sectional tile of the torus boundary on Fig.3, middle, where a crossing of the thickened link is depicted (two of the vertices of the tile are glued together underneath the overpass).

If we look at the Fig.3, left, we can write the expressions for the angles of the cross-section in terms of the diagram labels. Two opposite angles of the cross-section are $\arg \frac{u}{u+1}$ and $\arg \frac{-v}{-(v+1)}$ (the corresponding quadrilateral is depicted in Fig.4, left). The condition (a) allows to choose the solution to the hyperbolicity equations that is consistent with the orientation conventions used in the definitions of the diagram labels (when choosing out of two Galois conjugates). The consistency for the other labels follows automatically from the equations after the correct choice of the solution is made. Note that if $u = a + bi$ and $\text{Im } u = b > 0$, then $\text{Im} \frac{u}{u+1} = \frac{b}{(a+1)^2 + b^2} > 0$. Therefore, the condition (a) also guarantees that $\text{Im} \frac{u}{u+1}$ and $\text{Im} \frac{v}{v+1}$ are positive, and therefore $\arg \frac{u}{u+1}$ and $\arg \frac{v}{v+1}$ (corresponding to two opposite angles of the quadrilateral cross-section) are between 0 and π . In the case $\text{Im } u = b < 0$, $\text{Im} \frac{u+1}{u} = \text{Im} \frac{-b}{(a+1)^2 + b^2} > 0$, and the same angles are between 0 and π again. The condition (b) similarly guarantees that two other opposite angles of the cross-section are between 0 and π as well.

Consider a triangular cross-section (Fig.4, middle), resulted from collapsing a bigon region of the link diagram. If $\text{Im } u = b > 0$, then the interior angles correspond to $\arg \frac{u}{u+1}$, $\arg(u+1)$, $\arg -\frac{1}{u}$. The arguments of $\frac{u}{u+1}$, $u+1$, $-\frac{1}{u}$ are between 0 and π (since $\text{Im} \left(-\frac{1}{u}\right) = -b > 0$). If $\text{Im } u = b < 0$, then the interior angles correspond to $\arg \frac{u+1}{u}$, $\arg(-u)$, $\arg \frac{1}{u+1}$, and are between 0 and π again. Therefore, the conditions (a) and (b) together imply cross-sectional convexity of the Menasco's polyhedra.

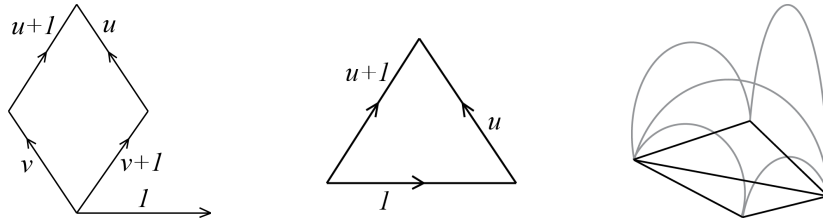


Fig.4

The condition (c) guarantees that we have at least four horospheres that are not all located in the same plane, since the quotient $\frac{w}{u_i v_j}$ is the cross-ratio of the centers of the corresponding horospheres (possibly, with a negative sign). For the details and proof, see Sections 2-4 in [15]. It also ensures that not all crossing labels are 0, which would force the system of hyperbolicity equations to be degenerate, of the form $0 = 0$. \square

We can now proceed to the main result of this section.

Proposition 3.2. Suppose that for an alternating link L there exists a solution to the hyperbolicity relations such that the conditions (a)–(c) are satisfied. Then each of ideal polyhedra Π_1, Π_2 is properly embedded in \mathbb{H}^3 , *i.e.* any two straightened faces either are identified, or are disjoint, or intersect in a connected sequence of edges (including the vertices that are the edges' endpoints), or in an ideal vertex only.

The rest of this section is devoted to the proof of the proposition. The proof consists of a number of observations about the geometric nature of the polyhedra.

Note that it is enough to prove the statement solely for the faces of Π_1 , since the construction of Π_2 is similar to that of Π_1 . Once the Proposition 3.2 holds for any two faces of Π_1 and any two faces of Π_2 , it holds for any pair of faces where one face is from Π_1 and the other face is from Π_2 by the construction as well.

By Lemma 3.1, Π_1 is cross-sectionally convex. This implies, in particular, that for any horosphere H centered at an ideal vertex v of Π_1 , the interior angles (not exterior) of the cross-section of Π_1 on H correspond to the dihedral angles of Π_1 in the horoball neighborhood of v bounded by H . It also implies that for any edge e of Q , the intersection of H and the interior of Π_1 is on one side of e (not on both), and is inside Q . Note also that the boundary of Π_1 is simply connected, and $\partial\Pi_1 - \{v\}$ is connected.

Lemma 3.3. Under the hypothesis of Proposition 3.2, there is no point p in $f(\partial\Pi_1 - \{v\})$ such that $f^{-1}(p)$ consists of at least two distinct points.

Proof of Lemma 3.3. Suppose the contrary.

Assume p is in the horoball neighborhood H of an ideal vertex of $\partial\Pi_1 - \{v\}$. Our definition of straightened faces implies that f is not bijective in such a horoball neighborhood in two cases. Firstly, if a face of Π_1 inside H is a piece of a vertical plane. But then this face of $\partial\Pi_1 - \{v\}$ has ∞ among its vertices, a contradiction. Secondly, if there are two faces of $\Pi_1 - \{v\}$ inside H , one directly above another. Since $\partial\Pi_1 - \{v\}$ is connected, this leads to two layers of faces, one above another, outside the horospherical neighborhood of the ideal vertex.

Now assume p is outside the horoball neighborhoods of ideal vertices of $\partial\Pi_1 - \{v\}$. Either two distinct points of $f^{-1}(p)$ belong to one triangle that is a part of straightened faces of Π_1 , or to two distinct triangles.

First, suppose distinct points from $f^{-1}(p)$ belong to the same triangle T of a face F . Since f is a vertical projection, this means that T is vertical as well (*i.e.* T is perpendicular to the plane $z = 0$). Recall that for the collection of vertices and straightened edges \dot{F} corresponding to the vertices and edges of a face of $\bar{\Pi}_1$, the triangulation is chosen so that every triangle projects bijectively under f , if such a triangulating exists. Such a triangulation does not exist only if there are two distinct consecutive edges of \dot{F} that lie in one vertical plane. Denote them by e_1, e_2 .

The edges e_1, e_2 are incident to an ideal vertex, say v , and there is the horosphere centered at v , say H . Denote the cusp cross-section of Π_1 on H by Q . Two vertices of Q that are on e_1, e_2 lie in the vertical plane. The other two vertices of Q must be outside the plane and on the same side from it to satisfy cross-sectional convexity. This implies that there are two levels of $\partial\Pi_1 - \{v\}$, one above another, on one side of T .

If two distinct points of $f^{-1}(p)$ do not belong to the same triangle, they belong to two different triangles, and there are two levels of $\partial\Pi_1 - \{v\}$, one above another, as well.

The assumption that there are two levels of faces of $\partial\Pi_1 - \{v\}$ leads to the following cases.

Case 1. A face of Π_1 incident to ∞ meets a face of the lower level, say (K_3, t_3) , and a face of the upper level, say (K_4, t_4) simultaneously at a certain vertex. We will denote the horosphere

centered at this vertex by H_{34} . This is depicted on Fig.5, left, with the faces of the upper level in black, and the faces of the lower level in grey (the triangulations of the faces are not pictured).

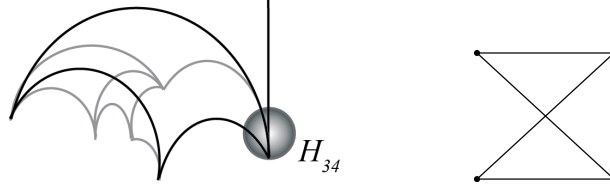


Fig.5

Two edges of $\mathcal{E}_i - v_i$ incident both to the center of H_{34} and to K_3 determine a plane that intersects H_{34} in an edge e . The vertices of the cross-section on H_{34} that are not the endpoints of e are on the opposite sides of the Euclidean line defined by e on H_{34} (Fig.5, right). This contradicts cross-sectional convexity.

Note that the same argument leads to a contradiction if at a vertex of $\partial\Pi_i - \{v\}$, faces of three or more levels meet. The same argument also gives a contradiction if two layers of faces meet at a edge e_p of \mathcal{E}_i , and the faces are adjacent to a single layer of faces at e_p .

Case 2. Faces meeting ∞ are incident at their vertices only to faces on the lower level. Denote a face with a vertex at ∞ by K_4 . Then we arrive at one of the two scenarios. Either K_4 has interior of the polyhedron on both sides near the plane $z = 0$ (as on Fig.7, left). Then on one of the horospheres adjacent to K_4 and not located at ∞ , the cross-section looks like Fig.5, right, again. A contradiction. In the second scenario, none of the faces, that are incident to ∞ and to lower level faces simultaneously, have interior of the polyhedron on both sides (as on Fig.7, right). Then the exterior angles of the cross-section correspond to the dihedral angles of the polyhedron in the corresponding horoball neighborhood of the vertex. A contradiction.

Case 3. Faces meeting ∞ meet only faces in the upper level at vertices. However there is a lower level of faces elsewhere. We then arrive at one of two scenarios. The first scenario is that the faces of upper and lower level meet at some edges of $\partial\Pi_i - \{v\}$ and are adjacent to a single layer of faces through those edges (and this single layer is then adjacent a face with a vertex at ∞). We then use the argument from case 1. The second scenario is to have a face with the vertex at ∞ adjacent to upper level of faces which then becomes a lower level. Then there is an ideal vertex q that is vertex of the face K_5 at least a part of which is in the upper level, and of the face K_6 at least a part of which is in the lower level. Denote the horosphere centered at q by H_{56} . K_5 intersects H_{56} in the edge e . Then the interior of the polyhedron is on both sides of e , since it is above the faces of the upper level adjacent to ∞ , and right above K_6 as well. A contradiction.

Case 4. Faces meeting ∞ meet a single layer of faces. Recall that the boundary of polyhedron is connected, and we have two layers of faces elsewhere. Hence the faces of upper and lower level either meet at some edges of $\partial\Pi_i - \{v\}$ and are adjacent to a single layer of faces at those edges, or intersect and switch levels. In the former situation, the argument from case 1 leads to a contradiction. In the latter situation, the argument from the second scenario of case 3 leads to a contradiction. \square

Corollary 3.4. The image of the edges of \mathcal{E}_i , $i = 1, 2$, that bound a face of Π_i under f is a simple polygon. Moreover, a restriction of f to every straightened face of Π_i is a bijection.

Proof of Proposition 3.2. If there are two distinct faces of $\partial\Pi_1 - \{v\}$ with intersecting interiors, then there is a point p in the image of one of the faces under f such that its preimage

consists of at least two distinct point. A contradiction to the claim.

Suppose there are two distinct faces K_1, K_2 of Π_1 , whose boundary intersects in more than just a vertex or a sequence of connected edges (as on Fig.6, left). K_1, K_2 result from a reduced and twist-reduced alternating diagram. Then Menasco's reduced alternating link diagram construction of the polyhedra implies that then there are two faces of D sharing more than a connected sequence of edges or a crossing. In a reduced and twisted-reduced alternating diagram, this is possible only if two adjacent non-bigon regions have a number of bigons between them, as in Fig.6, right, and share several crossings. But bigon are collapsed in Menasco's construction, and result in a row of consecutive edges in the corresponding polyhedra, that the faces share. A contradiction. \square

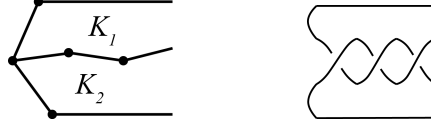


Fig.6

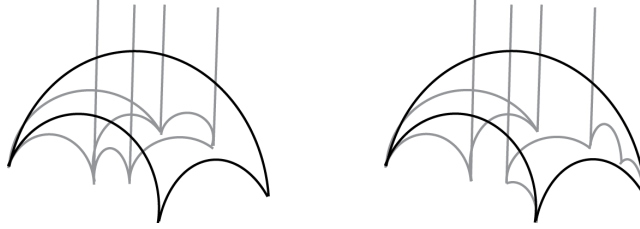


Fig.7

4. Ideal partially flat geodesic triangulations

Thurston provided sufficient conditions for an ideal triangulation of a finite volume 3-manifold to be geodesic, which can be expressed in gluing and completeness equations ([14]) together with a certain restriction on a solution. In particular, all the tetrahedra should have positive volume. Petronio and Weeks showed that this can also be achieved if an ideal triangulation is partially flat and satisfies the completeness and consistency conditions ([12]).

In this section, we will show that any cross-sectionally convex polyhedra in \mathbb{H}^3 can be subdivided into a partially flat geodesic triangulation. This implies that the conditions (a)–(c) guarantee the existence of the complete hyperbolic structure of $S^3 - L$, and the correspondence described in Section 2 induces a developing map.

Let us recall the nature of the conditions that make a triangulation an ideal geodesic partially flat triangulation. Consider a Euclidean cross-section of an ideal tetrahedron. Suppose that the (complex) translations corresponding to the sides of the cross-section are $u, v, -(u+v)$ (Fig.8). Any of $-\frac{v}{u}, \frac{u}{u+v}, \frac{u+v}{v}$ can be taken as the shape z of the tetrahedron (sometimes also called tetrahedral parameter or modulus), and their arguments correspond to the interior Euclidean angles of the cross-section, as well as to the interior dihedral angles of the tetrahedron.

Definition 4.1. The completeness and consistency conditions for an ideal triangulation τ are as follows.

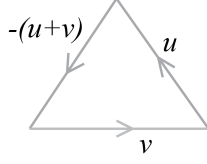


Fig.8

1) In every tetrahedron, three pairs of opposite edges correspond to z , $1 - \frac{1}{z}$, $\frac{1}{1 - z}$ in the way indicated above.

2) At every edge e of τ , after all the faces are identified in pairs, the shapes of the tetrahedra glued at e satisfy $z_1 z_2 \dots z_k = 1$.

3) For every tetrahedron, its shape z satisfies $\text{Im } z \geq 0$, and not all $z_i, i = 1, 2, \dots, n$ are 0.

4) The metric is complete, *i.e.* cross-sectional triangles glued together at each ideal vertex must fit together to give a closed Euclidean surface

Note that the condition $\arg z_1 + \arg z_2 + \dots + \arg z_k = 2\pi$ is often included (as a part of consistency conditions), but one can prove that if both (2) and (4) are satisfied, it is redundant.

Theorem 4.2. Suppose that for an alternating link L with the reduced alternating diagram D the edge and crossing labels satisfy the conditions (a)–(c). Then there exists a partially flat geodesic triangulation τ that induces the complete hyperbolic structure on $S^3 - L$.

Most of this section is devoted to the proof of the Theorem 4.2.

Under the hypothesis of the theorem, two straightened polyhedra Π_1, Π_2 that correspond to Menasco's decomposition of $S^3 - L$ are properly embedded in \mathbb{H}^3 by Prop 3.1. First, we construct a triangulation of $\Pi_1 \cup \Pi_2$ that is properly embedded in \mathbb{H}^3 . Recall that f is vertical projection described in the previous section. To begin, take the collection of ideal vertices and straightened edges \dot{F} corresponding to a face F of $\Pi_i - \{v\}$. Subdivide \dot{F} into (ideal) triangles using the existing ideal vertices of \dot{F} only. Additionally, do it so that for any new edge e subdividing \dot{F} of $\Pi_i - \{v\}, i = 1, 2$, $f(e)$ lies entirely in $f(F)$ (this can always be done as a consequence of Cor.3.3). Do this for every face of $\Pi_i - \{v\}, i = 1, 2$. Additionally, for every face F of $\Pi_i - \{v\}, i = 1, 2$, incident to ∞ , subdivide \dot{F} by edges incident to ∞ (*i.e.* by vertical geodesics from the other vertices of \dot{F}). Denote the resulting polyhedra with triangular faces by Π'_1, Π'_2 .

Recall that the faces of $\Pi_i, i = 1, 2$, do not have to be planar. Therefore, after we subdivided the faces in a new way, we have to check that the resulting polyhedra $\Pi'_i, i = 1, 2$, are properly embedded in \mathbb{H}^3 as well (*i.e.* the new triangular faces do not “cut” through each other). That is the content of the next lemma.

Fix i and consider a cross-section Q' of an ideal vertex of the polyhedron Π'_i resulting from the subdivision of faces of Π_i as above. Suppose Q' is situated on the horosphere H . Q' corresponds to the 4-sided cross-section Q of Π_i with the vertices A, B, C, D in the following way: Q' has the four vertices A, B, C, D of Q , and several more vertices resulting from the subdivision of faces of Π_i . We will refer to these vertices as to the “new” vertices of Q' .

Lemma 4.3. Suppose E is a new vertex of a cross-section Q' on a horosphere H . Suppose further E resulted from the subdivision of the face of Π_i that is incident to the edge CD of Q . Then either E lies either in the interior of Q , or on CD , or in the part of H bounded by the lines CD, AD, BC and on the other side of the line CD from AB (the area where E may lie is shown on Fig.9.)

Proof of Lemma 4.3. For a face F of Π_i , the image of any new edge subdividing \dot{F} under f lies entirely in the image of F .

Suppose first \dot{F} does not meet v . Since f is a homeomorphism on faces of $\Pi_i - \{v\}$ (by Proposition 3.2), any new edge of Π'_i resulting from the subdivision of \dot{F} does not intersect the interior of any face of Π_i besides F .

Now suppose \dot{F} has v among its vertices. Then the new edges resulting from the subdivision of \dot{F} are all vertical geodesics. Since there are no two levels of faces anywhere (see the proof of Lemma 3.3), these new edges do not pierce the interior of any face (besides F) as well.

Denote the geodesics that pierce H at the points A, B, C, D, E by $\alpha, \beta, \gamma, \delta, \eta$ respectively. If E lies outside the specified area, η pierces a face adjacent to either AD or AB or BC , a contradiction. \square

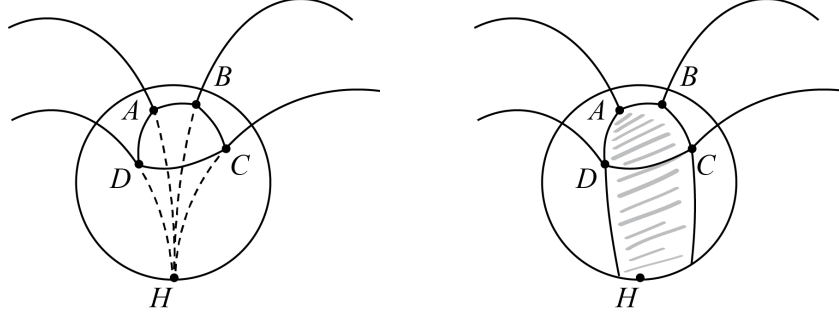


Fig.9

All the faces of Π'_1, Π'_2 are triangular faces, and the previous lemma implies that Π'_1, Π'_2 are properly embedded in \mathbb{H}^3 . We now will construct an ideal partially flat triangulation of Π'_1, Π'_2 , properly embedded in \mathbb{H}^3 .

Triangulate Π'_1, Π'_2 using the existing ideal vertices only, and so that the interiors of the triangular cross-sections of tetrahedra do not intersect. Denote such a triangulation by τ . Note that such τ always exists and is not unique; an example is the triangulation suggested by Thurston ([14]) and Menasco ([10]).

Lemma 4.4. Any tetrahedron in τ is either flat, or lies entirely inside the polyhedron, or lies entirely outside.

Proof of Lemma 4.4. The subdivision of cross-sections of Π'_i corresponds to the subdivision of the polyhedron Π'_i in the following way. Suppose we subdivided the cross-section Q' with the consecutive vertices A, B, C, D, E on the horosphere H by a new edge EC . Suppose P is the center of H . Suppose also that the vertices A, B, C, D, E result from geodesics $\alpha, \beta, \gamma, \delta, \eta$ respectively (as before) piercing H , and that these geodesics are edges of Π'_i . Then the plane P_{EC} defined by the geodesics γ, η intersects Q' in EC . Suppose also that P_1, P_2 are the ideal vertices that are adjacent to γ, η respectively on the sides opposite of P . We subdivide the cross-section Q' of Π'_i by an edge EC if we also subdivide Π'_i by a new triangular face that lies in the plane P_{EC} and has vertices P, P_1, P_2 (possibly with a new edge between P_1 and P_2).

After the triangulation process, all cross-sections of Π'_i are subdivided into triangles. If there is a tetrahedron T of τ that lies partially outside and partially in the polyhedron Π'_i in \mathbb{H}^3 , then at least one of the faces (say, a face F) of T is partially outside and partially in Π'_i . Then in the corresponding cross-section we have a subdividing edge that is partially inside and partially outside the cross-section, *i.e.* the subdividing edge intersects edges of the cross-section more than

just in their endpoints. This is not possible, since by Lemma 4.3 Q' is a simple polygon, and since by our construction the triangulation of Π'_i corresponds to triangulating this simple polygon. Similar argument shows that the interior of any truncated tetrahedron is not intersected by another truncated tetrahedron. \square

Proof of Theorem 4.2. Lemma 4.4 implies that τ is an ideal partially flat triangulation. Additionally, the condition (c) implies that not all tetrahedra have 0 volume (as explained in Lemma 3.1). Hence, the condition (3) from Definition 4.1 is satisfied. Now let us check the conditions (1), (2) and (4).

Let us look at the condition (2) of Definition 4.1. Choose an edge e of τ , and let T_1, \dots, T_k be tetrahedra glued at e . Their shapes are the ratios of the edge labels $z_1 = u_1/u_2$, $z_2 = u_2/u_3$, ..., $z_{k-1} = u_{k-1}/u_k$, $z_k = u_k/u_1$, where each u_i connects the point where e pierces H_1 with the points where other edges of T_1, T_2, \dots, T_k pierce H_1 (Fig.10, left). None of u_i is 0 due to the conditions (a)-(c), and the product of such shapes then satisfies $z_1 \dots z_k = 1$.

Turn our attention to the condition (1) of Definition 4.1. Consider a tetrahedron T in the triangulation τ . Suppose the (complex) translations corresponding to the sides of a cross-section lying at the horosphere H_1 are $u_1, v_1, -(u_1 + v_1)$. Let the geodesics of T be denoted by $\gamma_i, i = 1, 2, \dots, 5$ as on Fig.10, right. Then the shapes associated with the geodesics γ_1, γ_2 and γ_3 are $-\frac{v_1}{u_1}$, $\frac{u_1}{u_1 + v_1}$, $\frac{u + v}{v}$. Denote the first shape by z , and then the other two shapes are $1 - \frac{1}{z}$, $\frac{1}{1 - z}$. The corresponding Euclidean angles of the cross-section are arguments of the shapes, and so are three corresponding dihedral angles.

We need to check whether the opposite dihedral angles in T agree. For this, it is enough to check that the shapes agree. Suppose, another cross-section of T lying on the horosphere H_2 has sides $u_2, v_2, -(u_2 + v_2)$.

Diagram labels satisfy the region relations, and the relations are obtained by composing the isometries rotating (truncated) hyperbolic polygons. The polygons are preimages of the boundary of regions of D . We may use faces of a triangulation instead of the regions (the labels are defined so that they satisfy the relations coming from rotating these faces as well). All these faces are three-sided, which makes the relations particularly simple.

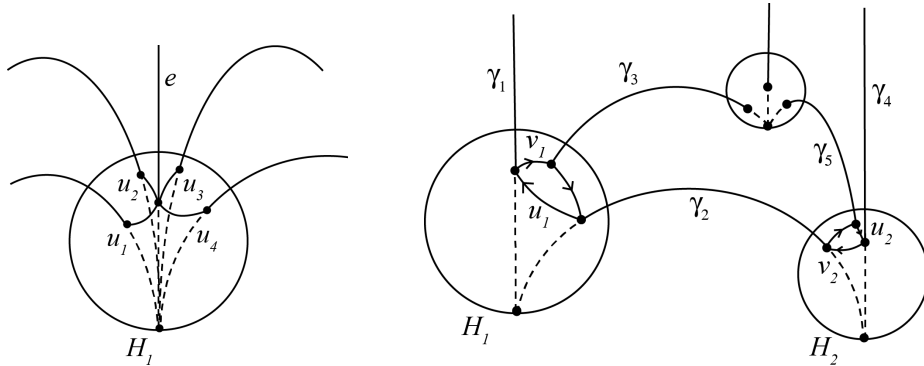


Fig.10

Let us show that the shape of T associated with γ_3 is equal to the shape of T associated with γ_4 . The former is $\frac{u_1 + v_1}{v_1}$, while the latter is $\frac{-v_2}{u_2}$.

From the 3-sided polygon that is a face of T determined by geodesics $\gamma_1, \gamma_2, \gamma_4$: $\frac{w_2}{u_1 v_1} = 1$, and therefore $v_2 = \frac{w_2}{u_1}$. From the 3-sided polygon, that is a face of T , determined by $\gamma_3, \gamma_2, \gamma_5$: $\frac{w_2}{(u_1 + v_1)(u_2 + v_2)} = 1$, and therefore $u_2 + v_2 = \frac{w_2}{u_1 + v_1}$. Then, from the cross-section of T on the horosphere H_2 , $u_2 = (u_2 + v_2) - v_2 = \frac{w_2}{u_1 + v_1} - \frac{w_2}{u_1}$.

Substitute the above expressions for v_2 and u_2 in the shape of T associated with γ_4 . After routine simplifications, we obtain $\frac{-v_2}{u_2} = -\frac{u_1 + v_1}{v_1}$, which is exactly the shape of T associated with γ_3 . Similarly one can show that other pairs of shapes of T agree.

Lastly, let us check the condition (4) of Definition 4.1, namely that Euclidean cross-sections of all tetrahedra incident to a particular ideal vertex v_1 of $\Pi_i, i = 1, 2$, form a closed Euclidean surface. The tetrahedra are glued at an ideal edge incident to v_1 , say e . Denote the other ideal vertex of e by v_2 . Denote the horosphere centered at v_1 by H_1 .

Recall that every ideal vertex of τ in \mathbb{H}^3 corresponds to an overpass or an underpass of the diagram D . Every edge connecting the vertices of τ lies on a geodesic that connects the centers of the corresponding horospheres. Hence, there is a quadrilateral cross-section of Π_i on H_1 resulting from connecting H_1 with four neighboring horospheres by four distinct arcs (Fig.11, left). Let u_1, u_2, u_3, u_4 be the corresponding edge labels as in the figure. Since u_1, u_2, u_3, u_4 satisfy the definition of the edge labels, they are determined by the Euclidean translations between the points where the corresponding arcs pierce H_1 .

Suppose first e is an edge of $\Pi_i, i = 1, 2$, then there is a vertex Q lying on e of the quadrilateral cross-section on H_1 . Three such cross-sections meet at Q as in the Fig.3, center. The edges of these cross-sections are u_1, u_2, u_3, u_4 by the definition of the edge labels and our construction of the polyhedra $\Pi_i, i = 1, 2$. Therefore, the cross-sections meet to form a closed Euclidean surface.

We triangulated $\Pi_1 \cup \Pi_2$ by adding more arcs (edges) between the existing ideal vertices. For an ideal vertex v_1 , all the arcs of the triangulation start at H_1 and end at one of the neighboring horospheres, which correspond to other overpasses and underpasses. Suppose now e is not an edge of $\Pi_i, i = 1, 2$, and was added in the triangulation process. Define u'_3 and u''_3 be complex numbers corresponding to the translations between the point where e pierces H_1 , and the points where the arcs immediately to the right and immediately to the left to e pierce H_1 . The numbers u'_3 and u''_3 are uniquely determined by the previous labels and the choice (and hence location on the plane $z = 0$) of the ideal vertices for the incident tetrahedra (in particular, $u'_3 + u''_3 = u_3$ as in Fig.11, right). Hence, the triangular cross-sections of all tetrahedra fit together to form a closed Euclidean surface.

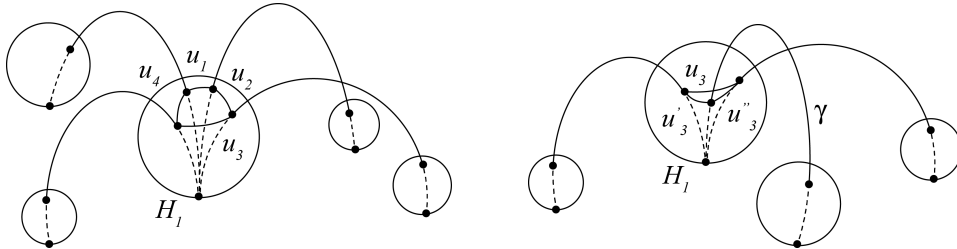


Fig.11

Since the conditions (1)-(4) are satisfied by τ , we may use Theorem 1.1 from [12] to state that the complete hyperbolic structure on $S^3 - L$ exists. \square

The diagram labels that satisfy the hyperbolicity equations and conditions (a)-(c) above were used to prove the existence of the complete hyperbolic structure on L . If, rather, we assume that the structure exists, we automatically obtain the following statement from our construction of a triangulation.

Corollary 4.5. Once a hyperbolic 3-manifold M has a decomposition into two ideal cross-sectionally convex polyhedra in \mathbb{H}^3 , there exists an ideal partially flat geodesic triangulation of M .

5. Isotopy classes of crossing arcs

The following statement provides a method for determining whether a crossing arcs is isotopic to a simple geodesic. Note that to check the conditions (a)-(c), one does not have to perform a decomposition of the link complement into polyhedra (or tetrahedra).

Theorem 5.1. Under the conditions (a)-(c) on the diagram labels of a reduced alternating diagram D of a link L , its crossing arcs are isotopic to simple geodesics.

Proof. The proof of Theorem 1.1 from [12] implies that the topological space obtained by gluing the tetrahedra (some, possibly, flat) is homeomorphic to $S^3 - L$, and that the hyperbolic structure of $S^3 - L$ locally induces its own metric on each tetrahedron. Therefore, the edges of τ are geodesics in \mathbb{H}^3 , and the tetrahedra of τ are isometric to the corresponding tetrahedra in $S^3 - L$, making the edges of the corresponding triangulation of $S^3 - L$ geodesics as well. By Thurston-Menasco construction of the polyhedra (that we later triangulated, obtaining τ), every crossing arc of D is an edge of τ .

Let us now check that the crossing arcs are simple geodesics, *i.e.* have no self-intersections. The only edges of τ that intersect in one point in \mathbb{H}^3 are two distinct edges of a flat tetrahedron (and, respectively, the edges that are identified with these two edges under the gluing). We need to check that these edges do not correspond to the same crossing arc in $S^3 - L$. By the Thurston-Menasco construction, a crossing arc c in $S^3 - L$ corresponds to one edge e_1 of Π_1 , and one edge e_2 of Π_2 . Under the gluing, e_1 and e_2 are identified, and therefore they cannot be two distinct edges of one geometric tetrahedron intersecting in just one point. \square

6. Examples and conclusions

The following examples illustrate that the conditions (a)-(c) are not too restrictive, and also show how to check them in practice. The first example is an infinite family of alternating braids, and the second one is an alternating link randomly chosen from the tables. To my knowledge, nothing was known about isotopy classes of their crossing arcs before. Empirical data suggests that many other hyperbolic alternating links satisfy the conditions (a)-(c).

Example 6.1. Consider an infinite family of alternating closed braids $(\sigma_1\sigma_3\sigma_2^{-1})^n$ and $(\sigma_1\sigma_3\sigma_2^{-1})^n\sigma_1\sigma_3$, $n > 1$. Fig.12, left, shows a fragment of such link with the diagram labels. The link can always be oriented as on the figure. Then the symmetry together with the relations for 3-sided region imply that there is only one edge label, u_1 , and all the crossing labels are $\pm w_1$, where the sign depends on whether the crossing is negative (as the crossings in the middle on Fig.12, left) or positive (as the leftmost and rightmost crossings on Fig.12, left).

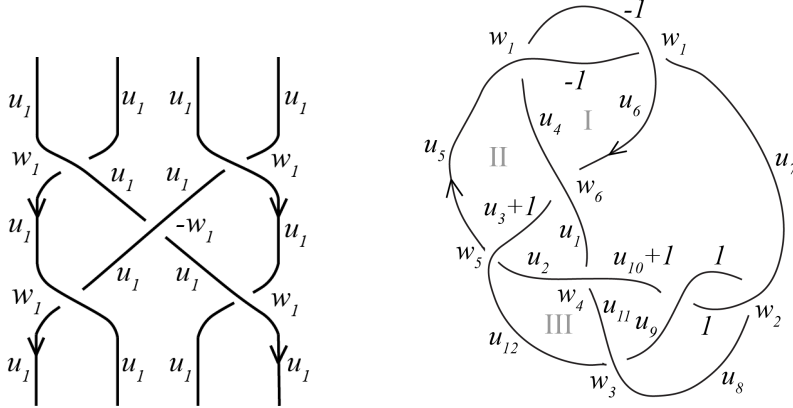


Fig.12

The shape (in the sense of [15]) of the regular n -sided region was established in [15] and is $\frac{w_1}{u_1^2} = \left(\frac{1}{2} \sec \frac{\pi}{n}\right)^2$. Then the labels that satisfy the conditions (a)-(c) are $w_1 = i/2$, $u_1 = (-1 - i)/2$.

The same argument applies to any alternating closed braid of the type $(\sigma_1 \sigma_3 \dots \sigma_{2k+1} \sigma_2 \sigma_4 \dots \sigma_{2k}^{-1})^n$, $n > 2$, showing that the crossing arcs of the reduced alternating diagram of such a link are isotopic to geodesics. Note that these are braids that have an even index. One may also use similar argument for closed alternating braids with no bigons of odd index, generalizing Example 6.2 from [15].

Example 6.2. Consider the 2-component link 8_8^2 in the Rolfsen table, and its reduced alternating diagram (Fig.12, right). Assign diagram labels and orientation to it as on the figure. Recall that every region yields three region relations. Below we give the relations, and the decimal values of the labels necessary to check the conditions (a)-(c). This simple calculation shows that all the crossing arcs are isotopic to geodesics.

From the regions I, II, III respectively:

$$\begin{aligned} w_1 + u_6 &= 0, & w_6 - u_6 u_4 &= 0, & w_1 + u_4 &= 0, & w_1 + (u_4 + 1)(u_5 + 1) &= 0, \\ w_5 - (u_5 + 1)(u_3 + 1) &= 0, & w_6 + (u_4 + 1)(u_3 + 1) &= 0, & w_5 - (u_{12} + 1)(u_2 + 1) &= 0, \\ w_4 - (u_2 + 1)(u_{11} + 1) &= 0, & w_3 - (u_{11} + 1)(u_{12} + 1) &= 0. \end{aligned}$$

From the other three 3-sided regions:

$$\begin{aligned} w_6 - u_3 u_1 &= 0, & w_4 + u_2 u_1 &= 0, & w_5 + u_2 u_3 &= 0, & w_2 - u_{10} u_9 &= 0, & w_3 + u_{11} u_9 &= 0, \\ w_4 + u_{10} u_{11} &= 0, & w_2 + u_8 + 1 &= 0, & w_3 - (u_8 + 1)(u_9 + 1) &= 0, & w_2 + u_9 + 1 &= 0. \end{aligned}$$

Lastly, of the two 5-sided regions (one of which is the outer region of the diagram), each yields equations of the form $\xi_1 \xi_3 - (\xi_1 + \xi_2 + \xi_3) + 1 = 0$, $\xi_2 \xi_4 - (\xi_2 + \xi_3 + \xi_4) + 1 = 0$, $\xi_3 \xi_5 - (\xi_3 + \xi_4 + \xi_5) + 1 = 0$, where for the inner region $\xi_1 = \frac{-w_1}{(u_6 + 1)(u_7 + 1)}$, $\xi_2 = \frac{-w_2}{u_7 + 1}$, $\xi_3 = \frac{-w_2}{u_{10} + 1}$, $\xi_4 = \frac{w_4}{(u_1 + 1)(u_{10} + 1)}$, $\xi_5 = \frac{-w_6}{(u_1 + 1)(u_6 + 1)}$, and for the outer $\xi_1 = \frac{-w_1}{u_7}$, $\xi_2 = \frac{w_2}{u_7 u_8}$, $\xi_3 = \frac{-w_3}{u_{12} u_8}$, $\xi_4 = \frac{-w_5}{u_{12} u_5}$, $\xi_5 = \frac{w_1}{-u_5}$.

One can then use a computer algebra system to obtain the solutions. The solution that satisfies the condition (a)-(c) has the following approximate decimal values of the labels: $w_1 = 0.37 - 0.52i$, $w_2 = -0.37 - 0.52i$, $w_3 = -0.13 + 0.39i$, $w_4 = 0.19 + 0.34i$, $w_5 = -0.19 + 0.34i$, $w_6 = -0.13 - 0.39i$, $u_1 = -0.08 + 0.63i$, $u_2 = -0.5 + 0.36i$, $u_3 = -0.58 + 0.27i$, $u_4 = u_6 = -0.37 + 0.52i$, $u_5 = -0.85 + 0.78i$, $u_7 = -0.5 + 1.9i$, $u_8 = u_9 = -0.63 + 0.52i$,

$u_{10} = -0.05 + 0.78i$, $u_{11} = -0.42 + 0.27i$, $u_{12} = -0.92 + 0.63i$. Therefore, the crossing arcs of the diagram on Fig.12, right, are isotopic to geodesics.

Determining isotopy classes of arcs is a difficult question on the geometry of 3-manifolds. The above conditions provide a simpler approach to this question for various families of alternating links. It is also of note that experimental data suggests the following conjecture.

Conjecture 6.3. The Thurston-Menasco ideal polyhedra in a hyperbolic alternating link complement in S^3 are cross-sectionally convex hyperbolic polyhedra, and the Thurston-Menasco ideal triangulation is a partially flat geodesic triangulation.

7. Acknowledgments

I am grateful to Marc Lackenby for many enlightening conversations and comments on the draft; to Marc Culler, David Futer, Joel Hass, Carlo Petronio, Jessica Purcell, and Abigail Thompson for helpful discussions. The work was partially supported by the NSF-AWM travel mentoring grant, and by the NSF DMS-1406588 grant.

References

- [1] Colin C. Adams, *Unknotting tunnels in hyperbolic 3-manifolds*, Math. Ann. 302 (1995), no. 1, 177–195.
- [2] Colin C. Adams, Alan W. Reid, *Unknotting tunnels in two-bridge knot and link complements*, Comment. Math. Helv. 71 (1996), no. 4, 617–627.
- [3] H. Akiyoshi, M. Sakuma, M. Wada, Y. Yamashita, *Ford domains of punctured torus groups and two-bridge knot groups*, Hyperbolic spaces and related topics, II (Japanese) (Kyoto, 1999). Srikaiseikikenkyusho Kkyroku No. 1163 (2000), 67–77.
- [4] S. D. Burton, J. S. Purcell, *Geodesic systems of tunnels in hyperbolic 3-manifolds*, Algebr. Geom. Topol. 14 (2014), no. 2, 925–952.
- [5] D. Cooper, D. Futer, J. Purcell, *Dehn filling and the geometry of unknotting tunnels*, Geom. Topol., Vol. 17 (2013), no. 3, 1815–1876.
- [6] F. Gueritaud, *On canonical triangulations of once-punctured torus bundles and two-bridge link complements*, with an appendix by D. Futer, Geom. Topol. 10 (2006), 1239–1284.
- [7] F. Gueritaud, *Geometrie hyperbolique effective et triangulations ideales cononiques en dimension 3*, Ph.D. thesis, L’Université de Paris (2006)
- [8] M. Lackenby, *The volume of hyperbolic alternating link complements*, with an appendix by I. Agol and D. Thurston., Proc. London Math. Soc. (3) 88 (2004), no. 1, 204–224.
- [9] M. Lackenby, *An algorithm to determine the Heegaard genus of simple 3-manifolds with nonempty boundary*, Algebr. Geom. Topol. 8 (2008) 911–934.
- [10] W. W. Menasco, *Polyhedra representation of link complements*, Low-dimensional topology (San Francisco, Calif., 1981), 305–325, Contemp. Math., 20, Amer. Math. Soc., Providence, RI, 1983.

- [11] C. Petronio, *An algorithm producing hyperbolicity equations for a link complement in S^3* , Geom. Dedicata 44 (1992), no. 1, 67–104.
- [12] C. Petronio, J. R. Weeks, *Partially flat ideal triangulations of cusped hyperbolic 3-manifolds*, Osaka J. Math. 37 (2000), 453–466.
- [13] M. Sakuma and J. R. Weeks, *Examples of canonical decomposition of hyperbolic link complements*, Japan. J. Math. (N. S.) 21 (1995), No. 2, 393–439.
- [14] W. P. Thurston, *The geometry and Topology of Three-Manifolds*, Electronic Version 1.1 (March 2002), <http://www.msri.org/publications/books/gt3m/>
- [15] M. Thistlethwaite, A. Tsvietkova, *An alternative approach to hyperbolic structures on link complements*, Algebr. Geom. Topol. 14 (2014), 1307–1337.
- [16] A. Tsvietkova, *Hyperbolic Structures from Link Diagrams*, Ph.D. thesis, University of Tennessee (2012).
- [17] J. R. Weeks, *SnapPea*: a computer program for creating and studying hyperbolic 3-manifolds, freely available from
<http://thames.northnet.org/weeks/index/SnapPea.html>

Anastasiia Tsvietkova
 Department of Mathematics
 University of California, Davis
 One Shields Ave, Davis, CA 95616, USA
 tsvietkova@math.ucdavis.edu